Experimental and Molecular Pathology 110 (2019) 104294

Contents lists available at ScienceDirect

Experimental and Molecular Pathology

journal homepage: www.elsevier.com/locate/yexmp

RHOA G17V mutation in angioimmunoblastic T-cell lymphoma: A potential biomarker for cytological assessment

Pei-Hang Lee[a,b,1], Shao-Wen Weng[c,1], Ting-Ting Liu[b], Huey-Ling You[a,d], Chun-Kai Liao[c], Ming-Chung Wang[c,2], Wan-Ting Huang[a,b,d,*,2]

[a] Department of Laboratory Medicine, Kaohsiung Chang Gung Memorial Hospital, Chang Gung University College of Medicine, Kaohsiung 83301, Taiwan
[b] Department of Pathology, Kaohsiung Chang Gung Memorial Hospital, Chang Gung University College of Medicine, Kaohsiung 833031, Taiwan
[c] Department of Internal Medicine, Kaohsiung Chang Gung Memorial Hospital, Chang Gung University College of Medicine, Kaohsiung 83301, Taiwan
[d] Department of Medical Laboratory Sciences and Biotechnology, Fooyin University, Kaohsiung 83102, Taiwan

ARTICLE INFO

Keywords:
Angioimmunoblastic T-cell lymphoma
Peripheral T-cell lymphoma
RHOA
Fine-needle aspiration cytology

ABSTRACT

Background: The World Health Organization, in a 2016 revision, introduced recurrent genetic abnormalities for classifying mature T- and NK-cell neoplasms. However, the role of genetic analyses from lymph node aspiration cytology is still not elucidated. We hypothesize that the use of genetic analyses may increase the accuracy of diagnosis from cytological preparations.

Methods: Fifty-seven formalin-fixed paraffin-embedded (FFPE) samples were collected for next-generation sequencing (NGS) targeting potential driver mutations including *TET2*, *DMN3TA*, *IDH2*, *RHOA*, *STAT3*, and *STAT5B*. Competitive allele-specific TaqMan polymerase chain reaction (cast-PCR) was performed to validate the mutation status by using FFPE and preoperative fine needle aspiration cytology (FNAC) samples.

Results: Among these six candidate genes, only *IDH2* and *RHOA* mutations were significantly more frequent in nodal subtypes, angioimmunoblastic T-cell lymphoma (AITL) and peripheral T-cell lymphoma, not otherwise specified (PTCL, NOS) ($P = .002$ and < 0.001, respectively). All genes exhibited different mutation patterns except *RHOA* with a hotspot mutation involving the Gly17 residue. The *RHOA* G17V mutation was found in 15 (75%) of 20 AITL and two (22%) of nine PTCL, NOS. Cast-PCR using FFPE samples showed 100% concordance with NGS. Among 12 lymph node aspirates, the preliminary diagnoses were suspicious for lymphoma (3, 25%), atypical lymphoid cells (3, 25%) and benign/negative (6, 50%). Cast-PCR detected the *RHOA* G17V mutation in six (75%) of eight *RHOA*-mutated aspirates and revealed negative results in all (100%) of four wild-type aspirates, with an 83.3% (10/12) concordance comparing to FFPE samples.

Conclusions: The *RHOA* G17V mutation serves as a useful biomarker for cytological assessment in AITL. The use of cast-PCR is valuable in the diagnosis of malignant lymphomas from cytological preparations, and thus avoiding the potential risks of invasive procedures.

Abbreviations: WHO, World Health Organization; H&E, hematoxylin and eosin; AITL, angioimmunoblastic T-cell lymphoma; PTCL, NOS, peripheral T-cell lymphoma, not otherwise specified; NKTCL, extranodal nasal-type NK/T-cell lymphoma; ITCL, intestinal T-cell lymphoma; ATLL, adult T-cell leukemia/lymphoma; FFPE, formalin-fixed paraffin-embedded; FNAC, fine-needle aspiration cytology; NGS, next-generation sequencing; PCR, polymerase chain reaction; VAF, variant allele frequency; TET2, ten-eleven translocation 2; DNMT3A, DNA-methyltransferase 3 alpha; IDH2, isocitrate dehydrogenase 2; RHOA, Ras homolog family member A; STAT, signal transducer and activator of transcription; TERT, telomerase reverse transcriptase; SH2, Src homology 2; GDP, guanosine diphosphate; GTP, guanosine-triphosphate; 2HG, 2-hydroxyglutarate; IL, interleukin; ECOG, Eastern Cooperative Oncology Group

* Corresponding author at: Department of Laboratory Medicine, Kaohsiung Medical Center, Chang Gung Memorial Hospital, 123, Ta-pei Road, Niao-Sung District, Kaohsiung City, Taiwan.

E-mail addresses: mr9244@cgmh.org.tw (P.-H. Lee), wengsw99@gmail.com (S.-W. Weng), liutt107@cgmh.org.tw (T.-T. Liu), youhling@cgmh.org.tw (H.-L. You), wangmt@cgmh.org.tw (M.-C. Wang), huangwanting5@gmail.com (W.-T. Huang).

[1] Shared first authorship.
[2] Shared corresponding authorship.

https://doi.org/10.1016/j.yexmp.2019.104294
Received 18 April 2019; Received in revised form 27 May 2019; Accepted 2 August 2019
Available online 05 August 2019
0014-4800/

1. Introduction

According to the 2016 revision of the World Health Organization (WHO) classification of lymphoid neoplasms (Swerdlow et al., 2016), recurrent genetic abnormalities have been introduced to classify mature T- and NK -cell neoplasms. Loss-of-function mutations affecting one or both copies of the ten-eleven translocation 2 (*TET2*) gene appear as an early event in the multistep lymphomagenesis process (Quivoron et al., 2011). An oncogenic cooperation between *TET2* and DNA-methyltransferase 3 alpha (*DNMT3A*) involving deregulation of cytosine methylation and demethylation processes has been proposed (Couronne et al., 2012). Another mutation, in isocitrate dehydrogenase 2 (*IDH2*), has also been reported to be frequently coexistent with mutations in *TET2* (Lemonnier et al., 2012). Nevertheless, activating mutations in signal transducer and activator of transcription 3 (*STAT3*) and *STAT5B* are exclusively identified in lymphomas derived from NK and γδ-T cells (Jerez et al., 2012; Koskela et al., 2012; Kucuk et al., 2015; Nicolae et al., 2014; Rajala et al., 2013). All the mutations involved in lymphomagenesis appear to be within the Src homology 2 (SH2) domain which mediates the dimerization and activation of proteins, and give rise to functionally active mutants that upregulate the expression of targeted genes (Kucuk et al., 2015).

In recent studies, the Ras homolog family member A (*RHOA*) G17V mutation is one of the most prevalent somatic mutations, which occurs in 50–70% of angioimmunoblastic T-cell lymphoma (AITL) and a smaller proportion of peripheral T-cell lymphoma, not otherwise specified (PTCL, NOS) (Palomero et al., 2014; Sakata-Yanagimoto et al., 2014; Yoo et al., 2014). RHOA is a GTPase that cycles between guanosine diphosphate (GDP)-bound inactive and guanosine-triphosphate (GTP)-bound active forms. The glycine at RHOA residue 17 is located at a critical position for GTP binding. The G17V RHOA protein is considered a loss-of-function mutant, as it does not bind Rhotekin, a molecule with high affinity for the GTP-bound form. This mutation is shown to induce autoimmunity and promote the development of AITL in transgenic mice (Cortes et al., 2018; Ng et al., 2018; Zang et al., 2017). The high frequency of the *RHOA* G17V mutation leads it a biomarker to follow the presence of AITL.

Previously, we had conducted a whole-exome sequencing study of *TP53* mutations and showed positive correlation of the mutation status with the immunostaining pattern in subtypes of peripheral mature T- and NK-cell lymphomas (Huang et al., 2018). In the present study, we aimed to examine mutations of *TET2*, *DNMT3A*, *IDH2*, *RHOA*, *STAT3*, and *STAT5B*, and figure out recurrent targets with high mutation rates for rapid diagnosis in clinical cytology. To this end, we first used the same cohort of 57 formalin-fixed paraffin-embedded (FFPE) samples to detect mutations by targeted gene sequencing. Furthermore, competitive allele-specific polymerase chain reaction (PCR) was performed on DNA materials extracted from both FFPE and fine-needle aspiration cytology (FNAC) samples to evaluate the applicability of cytology smear PCR.

2. Materials and methods

2.1. Patient samples

We included fifty-seven cases of peripheral mature T- and NK-cell lymphomas from the pathology files of Department of Pathology, Chang Gung Memorial Hospital at Kaohsiung, Taiwan during a 12-year period from 2006 to 2017, which were collected for our previous study (Huang et al., 2018). Two of the most common subtypes arising from the lymph node, AITL and PTCL, NOS were included. Extranodal nasal-type NK/T-cell lymphoma (NKTCL) and intestinal T-cell lymphoma (ITCL) were also enrolled, representing the extranodal subtypes. The available medical records and hematoxylin and eosin (H&E) stained sections were reviewed; H&E stained sections were classified according to the 2016 revision of the WHO classification of lymphoid neoplasms.

Table 1
Customized panels of targeted gene sequencing investigating hotspot regions.

Gene	Chromosome	Start	End	No. of primer pairs	Amplicon size (bp)
TET2	4	106,155,449	106,197,291	45	113–121
DNMT3A	2	25,457,236	25,469,933	8	116–125
IDH2	15	90,631,832	90,631,844	1	115
RHOA	3	49,412,962	49,412,978	1	119
STAT3	17	40,469,230	40,475,075	3	117–124
STAT5B	17	40,359,654	40,359,734	1	116

TET2, ten-eleven translocation 2; *DNMT3A*, DNA-methyltransferase 3 alpha; *IDH2*, isocitrate dehydrogenase 2; *RHOA*, Ras homolog family member A; *STAT3*, signal transducer and activator of transcription 3; *STAT5B*, signal transducer and activator of transcription 5B.

Preoperative FNAC samples were available in 9 AITL, 3 PTCL, NOS and 10 reactive lymphoid hyperplasia. This study was approved by the Ethics Committee of Chang Gung Memorial Hospital, Kaohsiung, Taiwan in accordance with the Declaration of Helsinki.

2.2. Customized targeted gene sequencing by next generation sequencing and bioinformatics analysis

Genomic DNA was amplified using customized panels designed by the Qiagen QIAseq designer website and next generation sequencing (NGS) data were analyzed as previously described (Huang et al., 2018). DNA libraries were prepared using QIAseq Targeted DNA Custom Panel Kit (QIAGEN, # CDHS-12087Z-81), purified using 1.0× Ampure beads and quantified using QIAseq Library Quant System (QIAGEN, Germany). The library was sequenced on an Illumina NextSeq (pair-end, 2 × 150 bp) following the manufacturer's user manual (Illumina, CA). The targeted mutations within six genes, including *TET2*, *DMN3TA*, *IDH2*, *RHOA*, *STAT3*, and *STAT5B* were listed in Table 1.

2.3. Detection of the RHOA G17V mutation by competitive allele-specific TaqMan PCR (cast-PCR)

DNA was collected from both FFPE and FNAC samples by using the QIAamp DNA Mini Kit (Qiagen, Hilden, Germany). The cytological material was scraped off the slide by scraping with a cell scraper. The *RHOA* G17V mutation was detected by cast-PCR on an ABI 7500 Fast qPCR machine (Thermo Fisher, CA, USA) with the following settings: 95 °C for 5 min, followed by 50 cycles of 95 °C for 3 s, and 60 °C for 40 s. Target was amplified in 10 μL reactions containing 10 ng of template DNA, 1× TopQ mutation Master Mix (Topgen Biotechology, Taiwan) and 1× of each TopQ Mutation Detection Assays (Topgen Biotechology). The qPCR mutation standards for absolute quantification were custom designed (Topgen Biotechology) (Table 2). The target mutation plasmids of 2500 copies, 500 copies, 50 copies and 5 copies were mixed with human gDNA 17 ng (5000 copies) to generate standards of 50%, 10%, 1% and 0.1% mutation frequency, respectively (Fig. 1). The telomerase reverse transcriptase (*TERT*) gene was used to monitor the amount of input sample DNA for qPCR to prevent overloading DNA templates, which might interfere with assay sensitivity and specificity. The linear regression model was used to evaluate the mutation variant allele frequency (VAF) of *RHOA* G17V, which was defined as positive if > 1%.

2.4. Statistical analysis

All statistical analyses were performed using SPSS for Windows 11.0 software (SPSS Inc. Chicago, IL, USA). The Fisher's exact test was used to compare the prevalence of targeted gene mutations between subtypes of peripheral mature T- and NK-cell lymphomas. All reported *P*

Table 2
Primers and probes used for detection of the *RHOA* G17V mutation.

Gene	Sequence (5′–3′)	Reference[a]	Amplicon (bp)
RHOA			
Primers			
RHOA-F	TGATGGAGCCTGTG T		
RHOA-R	GTGGGCACATACACCTCTGG	NC_000003.12	75
Wild-type blocker	AGCCTGTG G AAAG-MGB		
Probe	FAM-ATAGTCTTCAGCAAGGAC-MGB		
TERT			
Primers			
RHOA-F	AGGAATAGTCCATCCCCAGATTC		
RHOA-R	AGGGTCTCCACCTGGATGGT	NC_000005.10	88
Probe	HEX-TGCCCTCCTTTGCC-MGB		

[a] GRCh38.p12 (Genome Reference Consortium Human Build 38 patch release 12).

values are from two-tailed tests, and *P* values of 0.05 or less were considered to indicate statistical significance.

3. Results

3.1. Clinicopathological features and targeted gene sequencing

Fifty-seven cases, comprised of AITL (n = 20), PTCL, NOS (n = 9), NKTCL (n = 23), and ITCL (n = 5), were included in this study. More clinicopathologic findings are summarized as previously described (Huang et al., 2018).

A total of 27,359,085 mapped reads were generated, and 96% of the total bases were aligned to the complete human genome (Supplementary Tables 1 and 2). The median sequencing depth was 5289× (range: 850 to 18,079×). An average of 0.2× coverage uniformity accounted for > 99%. The cut-off value of VAF was settled at 5% for classifying cases as positive because the average number of molecular barcodes depth and read pairs per barcode conferred a confidence for calling 5% variants at 95% sensitivity.

IDH2 and *RHOA* mutations were significantly more frequent in nodal subtypes (P = .002 and < 0.001, respectively) (Table 3). For *TET2*, *DMN3TA*, *STAT3* and *STAT5B* mutations, no statistically significant differences between nodal and extranodal subtypes were identified. All genes exhibited different mutation patterns. However, the *RHOA* G17V mutation involving the Gly17 residue that participates in the GTP-binding was found in AITL (15/20; 75%) and PTCL, NOS (2/9; 22.2%). AITL samples with the *RHOA* G17V mutation had a VAF range from 2.0% to 30.6% (median: 11.8%). There was no significant correlation between the *RHOA* G17V mutation and clinicopathologic features (Supplementary Table 3). This mutation was validated and evaluated further for the molecular application in cytology.

3.2. Validation and detection of the RHOA G17 V mutation in FFPE and FNAC samples

The comparison of the *RHOA* G17V mutation detected by NGS and cast-PCR, and their use for FFPE and FNAC samples were summarized in Table 4. Twenty-five cases had enough tissue for further analysis of *RHOA* G17V following the NGS study. Cast-PCR showed 100% concordance with NGS using FFPE samples. FNAC from the involved lymph nodes were available in nine AITL and three PTCL, NOS cases. FNAC showed a heterogeneous population of hematolymphoid cells including small- to medium-sized lymphoid cells, histiocytes and follicular dendritic cells, and abundant lymphoglandular bodies in the background. The follicular dendritic cell meshwork was observed, which intimately admixed with lymphocytes to form a dendritic cell-lymphocyte complex (Fig. 2a). There were also lymphoid tissue fragments transgressing by arborizing blood vessels (Fig. 2b). The above features in cytologic preparations were reminiscent of those seen in histologic sections (Fig. 2c–h). There were three (25%) of 12 aspirates suspicious for lymphoma. Other preliminary diagnoses were atypical lymphoid cells (3, 25%) and benign/negative (6, 50%). Cast-PCR detected the *RHOA* G17V mutation in six (75%) of eight *RHOA*-mutated aspirates and revealed negative results in all (100%) of four wild-type aspirates, with an 83.3% (10/12) concordance comparing to FFPE samples (Table 4). No *RHOA* G17V mutation was detected in reactive lymphoid hyperplasia.

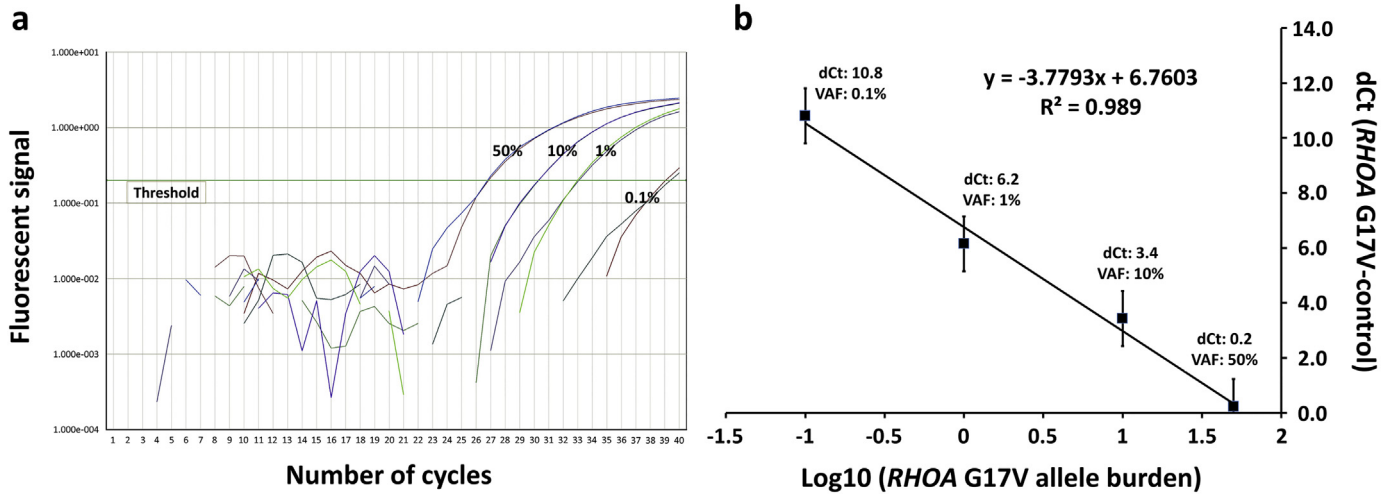

Fig. 1. Detection of the *RHOA* G17V mutation by competitive allele-specific TaqMan PCR (a) Amplification plot of target mutation plasmids of *RHOA* G17V showing the dynamic detection range of 4 orders of mutation frequency from 50% to 0.1% (average of cycles from left to right: 28.4, 31.7, 34.9 38.1, respectively). (b) The standard curve for determination of variant allele frequency (VAF) (R^2 = 0.989).

Table 3
The prevalence of targeted mutations in peripheral mature T and NK cell lymphomas.

Gene	Nodal subtypes			Extranodal subtypes					*P* value
	AITL (n = 20)		PTCL (n = 9)	NKTCL (*n* = 23)			ITCL (*n* = 5)		
TET2	4	(20.0%)	1	(11.1%)	3	(13.0%)	0	(0%)	0.706
DMN3TA	2	(10.0%)	2	(22.2%)	0	(0%)	1	(20.0%)	0.352
IDH2	8	(40.0%)	1	(11.1%)	0	(0%)	0	(0%)	0.002
RHOA	15	(75.0%)	2	(22.2%)	0	(0%)	0	(0%)	< 0.001
STAT3	0	(0%)	0	(0%)	2	(8.7%)	0	(0%)	0.237
STAT5B	0	(0%)	0	(0%)	0	(0%)	1	(20.0%)	0.491

TET2, ten-eleven translocation 2; *DNMT3A*, DNA-methyltransferase 3 alpha; *IDH2*, isocitrate dehydrogenase 2; *RHOA*, Ras homolog family member A; *STAT3*, signal transducer and activator of transcription 3; *STAT5B*, signal transducer and activator of transcription 5B; AITL, angioimmunoblastic T-cell lymphoma; PTCL, NOS, peripheral T-cell lymphoma, not otherwise specified; NKTCL, extranodal nasal-type NK/T-cell lymphoma; ITCL, intestinal T-cell lymphoma.

4. Discussion

We used NGS to clarify the prevalence of the targeted mutations in subtypes of peripheral mature T- and NK-cell lymphomas and uncovered the *RHOA* G17V mutation as a useful biomarker for cytological assessment in AITL. Some details of FNAC, including the follicular dendritic cell meshwork, arborizing vessels and mixed inflammatory cells may provide clues for AITL, which could be confirmed by integrating the *RHOA* G17V mutation analysis into clinical workflow. Given that only a minute fraction of lymph node FNAs will be obtained from AITL patients, the mutation analysis may be better performed by scraping the cytological material off the slides after cytological evaluation. The cytology smear PCR constitutes a sensitive and specific alternative to traditional diagnostic assays performed on biopsy specimens. It is a rapid, cost-effective, and noninvasive method for diagnosis and clinical follow-up of AITL, especially in patients with potential risks for invasive procedures.

For the past three decades, FNAC with flow cytometry (FCM) has been used in the evaluation of lymph nodes, and provided relevant information for the diagnosis, classification and monitoring of lymphoproliferative disorders. FCM immunophenotyping showed a high efficiency in the distinction between reactive processes and non-Hodgkin lymphomas (NHLs) with a false-positive rate of 4.7% (Savage et al., 2011). Further subclassification of lymphomas into WHO categories has been also improved, especially for low-grade B cell lymphomas (Bangerter et al., 2007; Barrena et al., 2011; Schmid et al., 2011). However, despite a general high sensitivity in clonality assessment, discrepant results between FCM and conventional histology are still present, ranging from 51 to 95% (Barrena et al., 2011; Peluso et al., 2016).

PCR-based molecular tests are particularly helpful when reporting the FNAC not only as a malignant lymphoma but also some specific

Table 4
Comparison of *RHOA* G17V mutation between FNAC and FFPE samples.

Case No.	FNAC diagnosis	FFPE diagnosis	*RHOA* G17V mutation			
			FNAC (PCR)	FFPE (PCR)	FFPE, VAF% (NGS)	
1	NA	AITL	NA	+	+	, 10.9
2	Benign/negative	AITL	−[a]	+	+	, 10.3
3	Atypical lymphoid cells	AITL	+	+	+	, 8.9
4	Suspicious for lymphoma	AITL	+	+	+	, 28.4
5	Benign/negative	AITL	+	+	+	, 9.5
6	NA	AITL	NA	−	−	, 0
7	Atypical lymphoid cells	AITL	+	+	+	, 13.1
8	Benign/negative	AITL	−	−	−	, 0
9	NA	AITL	NA	+	+	, 13.9
10	NA	AITL	NA	−	−	, 3.2
11	NA	AITL	NA	+	+	, 18.0
12	Atypical lymphoid cells	AITL	+	+	+	, 26.3
13	NA	AITL	NA	+	+	, 9.7
14	NA	AITL	NA	+	+	, 12.2
15	Benign/negative	AITL	+	−	–	, 2.0
16	Benign/negative	AITL	−	+	+	, 11.3
17	NA	AITL	NA	+	+	, 30.6
18	NA	AITL	NA	+	+	, 17.8
19	NA	AITL	NA	+	+	, 6.7
20	NA	AITL	NA	−	−	, 3.8
21	NA	PTCL	NA	NA	−	, 0
22	Suspicious for lymphoma	PTCL	−	−	−	, 0
23	NA	PTCL	NA	NA	−	, 0
24	NA	PTCL	NA	NA	−	, 0
25	NA	PTCL	NA	+	+	, 6.3
26	Benign/negative	PTCL	−	−	−	, 0
27	NA	PTCL	NA	+	+	15.2
28	Suspicious for lymphoma	PTCL	−	−	−	, 0
29	NA	PTCL	NA	NA	−	, 0

[a] Low DNA concentration (2.7 ng/μl) FNAC, fine-needle aspiration cytology; FFPE, formalin-fixed paraffin-embedded; AITL, angioimmunoblastic T-cell lymphoma; PTCL, NOS, peripheral T-cell lymphoma, not otherwise specified; PCR, polymerase chain reaction; NGS, next-generation sequencing; VAF, variant allele frequency.

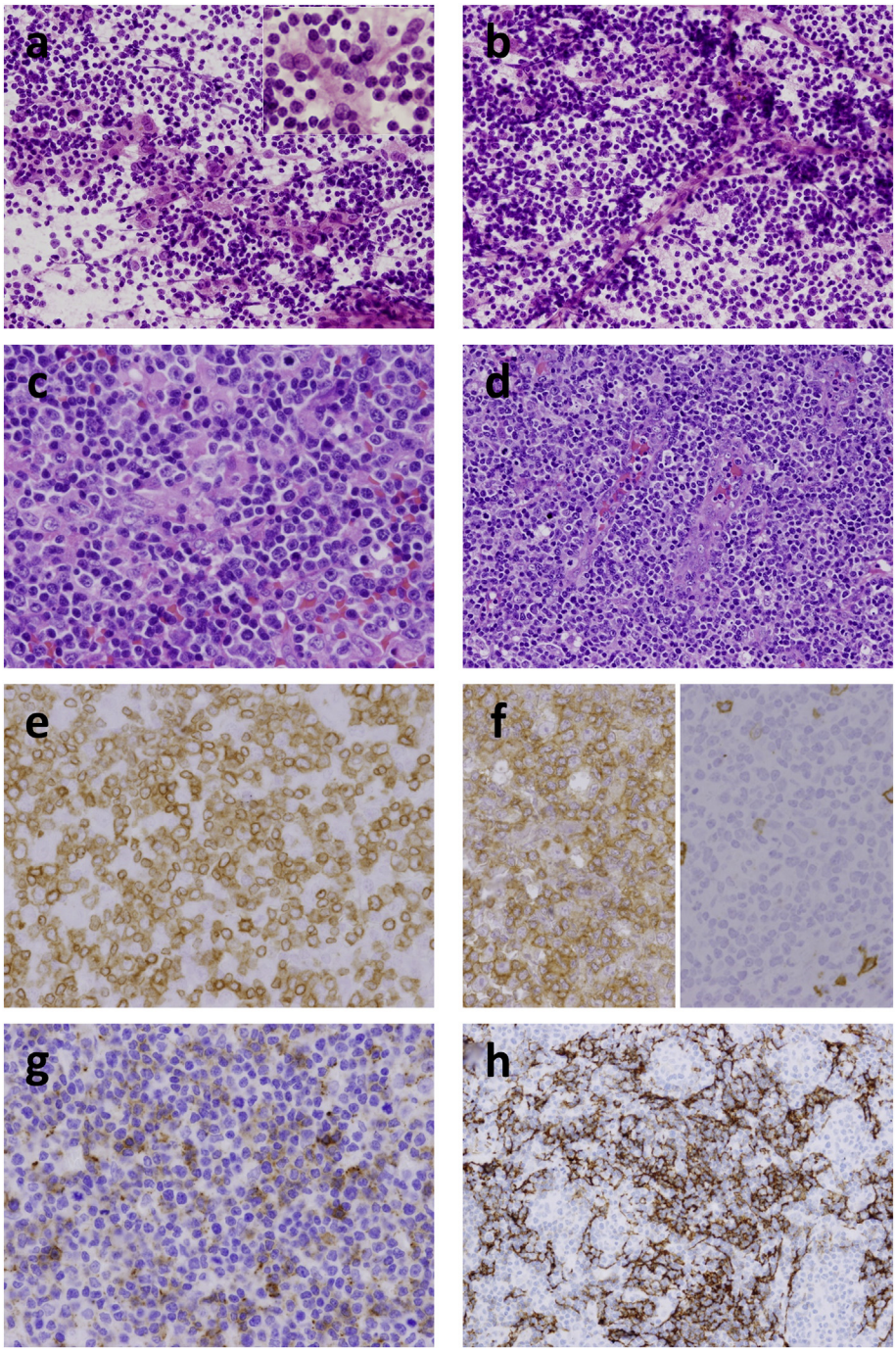

Fig. 2. Cytologic and histologic features of angioimmunoblastic T-cell lymphoma (Case 16). Cytologic smear showed (a) aggregates of follicular dendritic cells intimately admixed with lymphocytes, forming dendritic cell-lymphocyte complexes. Lymphoglandular bodies were seen in the background (H&E, magnification 200×). (upper right inset) After high-power examination of the smears, the follicular dendritic cells were characterized by "kissing nuclei," with finely dispersed chromatin and small central nucleoli (H&E, magnification 400×). (b) There were lymphoid tissue fragments containing a scaffold of arborizing blood vessels (H&E, magnification 200×). Histological sections showed (c) the typical appearance of an AITL composed of variably sized atypical lymphocytes with abundant follicular dendritic cells (H&E, magnification, 400×), and (d) the proliferation of high endothelial venules (H&E, magnification 200×). The neoplastic T cells were positive for (e) CD3, (f) (left) CD4, and (g) PD1, but negative for (f) (right) CD8 (magnification 400×). (h) The expanded follicular dendritic cell meshwork was highlighted by CD21 (magnification 200×).

NHL subtypes. Reverse transcription-PCR has been successfully applied on FNAC to detect specific chromosome translocations in B-cell NHLs. For T-cell NHLs, T-cell receptor (TCR) gene rearrangement is the mostly applied target for clonality testing, but not for further subclassification of lymphomas into WHO categories. The accuracy of this test is limited by the restricted diversity of TCR gamma gene rearrangements, high level of background noise amplification, and lack of clone quantification or immunophenotypic characterization (Novikov et al., 2019). Given the high frequency of *RHOA* G17V mutation in AITL, detection of the mutation may add clinical value of FNAC for subclassification of T-cell NHLs. However, inadequate sampling or a background of abundant mixed inflammatory cells may limit the detection of the monoclonal population (Venkatraman et al., 2006). In our study, there was discordance in the assessment of clonality by the *RHOA* G17V mutation between FNAC and FFPE samples in 2 of 12 (16.7%) cases. Case 2 had a low DNA concentration indicating a limited amount of material available from the aspirate. Case 16 showed tumor heterogeneity with abundant polyclonal cells limiting mutation detection in FNAC. These were possible causes of false-negative results. Repeat sampling may overcome the above limitations and increase the sensitivity of the aspirational biopsy.

RHOA-mutated AITL was clinically characterized by a higher incidence of splenomegaly and B symptoms, higher serum interleukin (IL)-2R, and a poorer Eastern Cooperative Oncology Group (ECOG) performance status than wild-type cases (Nagao et al., 2016; Ondrejka et al., 2016). It was also associated with pathologic features such as a higher mean microvessel density, a wider distribution of follicular dendritic cell networks, and a greater expression of follicular helper T-

cell markers. There was no difference in the overall survival between *RHOA*-mutated and -wild-type subgroups. Ondrejka et al. demonstrated that the median VAF was 14%, with a wide range of 0.4 to 50%, in *RHOA* G17V-mutated AITL without clarifying the significance of this mutational burden clinicopathologically (Ondrejka et al., 2016). In our study, we also found a wide range of *RHOA* G17V mutation VAF in tumors, while no significant correlation between the VAF and clinicopathologic features was identified. More studies with larger samples sizes are needed to establish if any relationship exists.

Aside from AITL, recent genetic studies have identified *RHOA* mutations in lymphoid malignancies such as adult T-cell leukemia/lymphoma (ATLL) (Kataoka et al., 2015; Nagata et al., 2016), Burkitt's lymphoma (Abate et al., 2015; O'Hayre et al., 2016; Richter et al., 2012; Rohde et al., 2014), and diffuse large B-cell lymphoma (O'Hayre et al., 2016), as well as in diffuse-type gastric carcinoma (Kakiuchi et al., 2014; Lawrence et al., 2014; Network, 2014; Ushiku et al., 2016; Wang et al., 2014) and other solid tumors (Lawrence et al., 2014). The mutations were widely distributed with some clearly targeted to the GTP-binding pocket. For instance, p.Cys16Arg was most frequent in ATLL (Nagata et al., 2016), whereas p.Arg5Gln and p.Tyr42Cys were most frequent in Burkitt's lymphoma (O'Hayre et al., 2016; Richter et al., 2012; Rohde et al., 2014) and gastric carcinomas (Kakiuchi et al., 2014; Network, 2014; Wang et al., 2014), respectively. The *RHOA* mutation encoding p.Thr19Ile was reported in PTCL by Palomero et al. (2014) and in ATLL by Nagata et al. (2016). The gain-of-function and loss-of-function *RHOA* mutations were even observed in the same disease category (Nagata et al., 2016). The biochemical activity of RHOA differs with each hotspot position. That may explains why different hotspot mutations dominate in different tumor subtypes (Ishikawa, 2016).

IDH2 R172 mutations were identified in 8 (40%) AITL cases in our study. The overall frequency of *IDH2* R172 mutations in AITL was previously reported to range from 13.8% to 45% (Cairns et al., 2012; Odejide et al., 2014; Wang et al., 2015). Substitution of this hotspot arginine residue is reported to cause the accumulation of the oncometabolite 2-hydroxyglutarate (2HG), which can inhibit α-ketoglutarate-dependent dioxygenases involved in histone methylation, hypoxia response, and collagen maturation, and contribute to the oncogenic process in AITL (Lemonnier et al., 2016). Further validation is necessary for this mutation as a biomarker in the molecular application of cytology.

In conclusion, the *RHOA* G17V mutation is a useful biomarker for cytological assessment in AITL because of the high frequency of the mutation. Patients with potential risks for invasive procedures can be followed by cytology smear PCR, which is rapid, cost-effective, and noninvasive.

Supplementary data to this article can be found online at https://doi.org/10.1016/j.yexmp.2019.104294.

Funding sources

This study was supported by the Chang Gung Memorial Hospital [grant number CMRPG8F1241 and CMRPG8F1242].

Declaration of Competing Interest

None.

Acknowledgments

We thank Hsuan-Ying Huang for a number of comments on the manuscript.

References

Abate, F., et al., 2015. Distinct viral and mutational spectrum of endemic Burkitt lymphoma. PLoS Pathog. 11, e1005158.
Bangerter, M., et al., 2007. Fine needle aspiration cytology and flow cytometry in the diagnosis and subclassification of non-Hodgkin's lymphoma based on the World Health Organization classification. Acta Cytol. 51, 390–398.
Barrena, S., et al., 2011. Flow cytometry immunophenotyping of fine-needle aspiration specimens: utility in the diagnosis and classification of non-Hodgkin lymphomas. Histopathology. 58, 906–918.
Cairns, R.A., et al., 2012. IDH2 mutations are frequent in angioimmunoblastic T-cell lymphoma. Blood. 119, 1901–1903.
Cortes, J.R., et al., 2018. RHOA G17V induces T follicular helper cell specification and promotes lymphomagenesis. Cancer Cell 33, 259–273.e7.
Couronne, L., et al., 2012. TET2 and DNMT3A mutations in human T-cell lymphoma. N. Engl. J. Med. 366, 95–96.
Huang, H.S., et al., 2018. TP53 mutations in peripheral mature T and NK cell lymphomas: a whole-exome sequencing study with correlation to p53 expression. Hum. Pathol. 80, 145–151.
Ishikawa, S., 2016. Opposite RHOA functions within the ATLL category. Blood 127, 524–525.
Jerez, A., et al., 2012. STAT3 mutations unify the pathogenesis of chronic lymphoproliferative disorders of NK cells and T-cell large granular lymphocyte leukemia. Blood 120, 3048–3057.
Kakiuchi, M., et al., 2014. Recurrent gain-of-function mutations of RHOA in diffuse-type gastric carcinoma. Nat. Genet. 46, 583–587.
Kataoka, K., et al., 2015. Integrated molecular analysis of adult T cell leukemia/lymphoma. Nat. Genet. 47, 1304–1315.
Koskela, H.L.M., et al., 2012. Somatic STAT3 mutations in large granular lymphocytic leukemia. N. Engl. J. Med. 366, 1905–1913.
Kucuk, C., et al., 2015. Activating mutations of STAT5B and STAT3 in lymphomas derived from gammadelta-T or NK cells. Nat. Commun. 6, 6025.
Lawrence, M.S., et al., 2014. Discovery and saturation analysis of cancer genes across 21 tumour types. Nature. 505, 495–501.
Lemonnier, F., et al., 2012. Recurrent TET2 mutations in peripheral T-cell lymphomas correlate with TFH-like features and adverse clinical parameters. Blood. 120, 1466–1469.
Lemonnier, F., et al., 2016. The IDH2 R172K mutation associated with angioimmunoblastic T-cell lymphoma produces 2HG in T cells and impacts lymphoid development. Proc. Natl. Acad. Sci. U. S. A. 113, 15084–15089.
Nagao, R., et al., 2016. Clinicopathologic analysis of angioimmunoblastic T-cell lymphoma with or without RHOA G17V mutation using formalin-fixed paraffin-embedded sections. Am. J. Surg. Pathol. 40, 1041–1050.
Nagata, Y., et al., 2016. Variegated RHOA mutations in adult T-cell leukemia/lymphoma. Blood. 127, 596–604.
Network, C. G. A. R, 2014. Comprehensive molecular characterization of gastric adenocarcinoma. Nature 513, 202–209.
Ng, S.Y., et al., 2018. RhoA G17V is sufficient to induce autoimmunity and promotes T-cell lymphomagenesis in mice. Blood. 132, 935–947.
Nicolae, A., et al., 2014. Frequent STAT5B mutations in gammadelta hepatosplenic T-cell lymphomas. Leukemia. 28, 2244–2248.
Novikov, N.D., et al., 2019. Utility of a simple and robust flow cytometry assay for rapid clonality testing in mature peripheral T-cell lymphomas. Am. J. Clin. Pathol. 151, 494–503.
Odejide, O., et al., 2014. A targeted mutational landscape of angioimmunoblastic T-cell lymphoma. Blood. 123, 1293–1296.
O'Hayre, M., et al., 2016. Inactivating mutations in GNA13 and RHOA in Burkitt's lymphoma and diffuse large B-cell lymphoma: a tumor suppressor function for the Galpha13/RhoA axis in B cells. Oncogene 35, 3771–3780.
Ondrejka, S.L., et al., 2016. Angioimmunoblastic T-cell lymphomas with the RHOA p.Gly17Val mutation have classic clinical and pathologic features. Am. J. Surg. Pathol. 40, 335–341.
Palomero, T., et al., 2014. Recurrent mutations in epigenetic regulators, RHOA and FYN kinase in peripheral T cell lymphomas. Nat. Genet. 46, 166–170.
Peluso, A.L., et al., 2016. Lymph node fine-needle cytology: beyond flow cytometry. Acta Cytol. 60, 372–384.
Quivoron, C., et al., 2011. TET2 inactivation results in pleiotropic hematopoietic abnormalities in mouse and is a recurrent event during human lymphomagenesis. Cancer Cell 20, 25–38.
Rajala, H.L., et al., 2013. Discovery of somatic STAT5b mutations in large granular lymphocytic leukemia. Blood 121, 4541–4550.
Richter, J., et al., 2012. Recurrent mutation of the ID3 gene in Burkitt lymphoma identified by integrated genome, exome and transcriptome sequencing. Nat. Genet. 44, 1316–1320.
Rohde, M., et al., 2014. Recurrent RHOA mutations in pediatric Burkitt lymphoma treated according to the NHL-BFM protocols. Genes Chromosomes Cancer 53, 911–916.
Sakata-Yanagimoto, M., et al., 2014. Somatic RHOA mutation in angioimmunoblastic T cell lymphoma. Nat. Genet. 46, 171–175.
Savage, E.C., et al., 2011. Independent diagnostic accuracy of flow cytometry obtained from fine-needle aspirates: a 10-year experience with 451 cases. Am. J. Clin. Pathol. 135, 304–309.
Schmid, S., et al., 2011. Flow cytometry as an accurate tool to complement fine needle aspiration cytology in the diagnosis of low grade malignant lymphomas. Cytopathology 22, 397–406.
Swerdlow, S.H., et al., 2016. The 2016 revision of the World Health Organization classification of lymphoid neoplasms. Blood 127, 2375–2390.
Ushiku, T., et al., 2016. RHOA mutation in diffuse-type gastric cancer: a comparative clinicopathology analysis of 87 cases. Gastric Cancer 19, 403–411.
Venkatraman, L., et al., 2006. Role of polymerase chain reaction and immunocytochemistry in the cytological assessment of lymphoid proliferations. J. Clin.

Pathol. 59, 1160–1165.
Wang, K., et al., 2014. Whole-genome sequencing and comprehensive molecular profiling identify new driver mutations in gastric cancer. Nat. Genet. 46, 573–582.
Wang, C., et al., 2015. IDH2R172 mutations define a unique subgroup of patients with angioimmunoblastic T-cell lymphoma. Blood 126, 1741–1752.
Yoo, H.Y., et al., 2014. A recurrent inactivating mutation in RHOA GTPase in angioimmunoblastic T cell lymphoma. Nat. Genet. 46, 371–375.
Zang, S., et al., 2017. Mutations in 5-methylcytosine oxidase TET2 and RhoA cooperatively disrupt T cell homeostasis. J. Clin. Invest. 127, 2998–3012.